

Activity Report of the “Electronic Structure” group (2017-2019)

We focus our research on the investigation of the electronic structure of catalysts and electrode surfaces used in heterogeneous catalytic reactions and electrochemical processes like propylene epoxidation over Ag, the oxygen evolution reaction (OER) and the CO₂ reduction reaction (CO₂RR). The development of electrochemical cells enabling operando X-ray absorption spectroscopy and X-ray photoelectron spectroscopy in the soft X-ray range is an essential part of our work [1-4].

IrO_x in OER

In case of Ir anodes in OER a strong hybridization between iridium and oxygen leads to holes shared between the two; the further the material is charged, the more charge transfer from iridium to the oxygen ligand is expected [2]. Depending on its coordination, oxygen can ultimately end up as a radical oxyl species, $\mu_1\text{-O}$. Such a species was proposed to be highly active in O-O bond formation [5]. We were able to find that species under wet conditions via its O K-edge absorption signal. A small amount appeared at the onset of the OER. Calculations and experiments are in good agreement about the deprotonation potentials and the O K-edge absorption energies of the considered surface

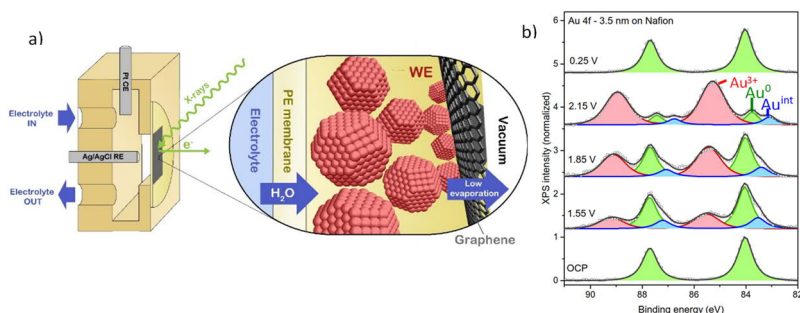


Figure 1: a) Cell design. b) In situ XPS spectra recorded with 0.1 M H₂SO₄ electrolyte.

oxygen species.

To probe active electrocatalyst surfaces in a liquid environment, we have developed an XPS/XAS cell in which the catalyst is confined between a proton exchange membrane and graphene. While the proton exchange membrane supplies a steady flow of electrolyte to the electrode, the X-ray and electron-transparent graphene layer greatly reduces the evaporation of water into the NAP-XPS chamber. Using O K-edge spectra, we confirmed that this can lead to the formation of a thin layer of liquid electrolyte between the graphene and the membrane. Thus, electrocatalysts can be studied under operating conditions using surface sensitive soft X-ray XPS and XAS [3,4].

With this methodology, we have studied the potential-driven restructuring of Ru, Pt and Au oxides in 0.1 M H₂SO₄ during the oxygen evolution reaction. Using Ru 3d/M-edge, Pt 4f and Au 4f spectra, we identified the distribution of cationic oxidation states as a function of potential (e.g. Figure 1b). For Au

oxide, which is strongly covalent, only Au^{3+} is found, whereas the more oxophilic Pt displays a gradual transition from Pt^0 to $\text{Pt}^{\delta+}/\text{Pt}^{2+}/\text{Pt}^{4+}$ and further to Pt^{4+} [4]. For the yet more oxophilic RuO_x , we find a gradual oxidation to primarily Ru^{4+} under OER conditions, with some minor contributions of higher oxidation states.

O K-edge spectra, complemented by theory, indicate that the final stages of oxidation of the catalysts occur through deprotonation, even in the bulk of the materials. The deprotonation proceeds through multiple stages: hydroxyl groups with higher coordination deprotonate at lower potential. Interestingly, we find that deprotonation is not complete during the oxygen evolution reaction on Ru oxide, in contrast to *ab initio* thermodynamic predictions [6].

Several studies have identified that the degree of crystallinity of OER electrodes influence their activity and stability [7]. Our in situ studies suggest that the reactive (deprotonated) oxygen species that dominate the surface of amorphous and crystalline Ru oxides under OER conditions are similar in nature. Rather, we explain the correlation between crystallinity and activity/stability by the larger amount of reactive species on amorphous electrodes.

CuO_x in CO₂RR

Copper is unique due to its ability to electro-reduce CO_2 to hydrocarbons and alcohols in aqueous electrolytes, as was probed by Hori et al [8]. Nevertheless, the selective electroreduction of CO_2 into fuels is challenging due to the multiple complex proton-coupled electron transfer steps that must occur [9]. This complex network makes the cathodic CO_2 reduction reaction (CO_2RR) run with relative low current density and high overpotential and in addition electrode deactivation may occur over time. By tracking the electronic structure of the Cu catalysts, using in situ X-ray spectroscopies, we have tuned and precisely set the initial Cu redox state, such as Cu^0 , Cu^+ and Cu^{2+} , by controlled applied potential protocols [10]. It was shown, that the magnitude of the CO_2 dissociation barrier depends on the degree of surface oxidation and on the nature of surface defects. Therefore, we calculated the barrier associated with dissociative CO_2 adsorption on several copper catalysts, indicating that the dissociation barrier is lowered in the presence of missing oxygen on the surface and enhanced in presence of extra oxygen on the surface.

Propylene Epoxidation over Ag

We used near ambient pressure X-ray photoelectron spectroscopy (NAP-XPS) to study the Ag surface under propylene epoxidation conditions. Opposed to ethylene epoxidation, $\text{SO}_{4,\text{ads}}$ is not present under steady state propylene oxidation conditions. $\text{SO}_{4,\text{ads}}$ can, however, be formed by introducing an SO_2 pulse to the reaction feed, resulting in an increase in selectivity to PO. Though, $\text{SO}_{4,\text{ads}}$ is rapidly titrated under reaction conditions and PO selectivity decreases with time following the decrease in $\text{SO}_{4,\text{ads}}$ coverage. During this process we observe the formation of $\text{SO}_{3,\text{ads}}$. As for ethylene epoxidation, it seems that $\text{SO}_{4,\text{ads}}$ is also responsible for propylene epoxidation and $\text{SO}_{3,\text{ads}}$ is seen as a titration product. However, NAP-XPS demonstrates atomic O has a low coverage under propylene epoxidation conditions compared to those for ethylene epoxidation. As a consequence, $\text{SO}_{4,\text{ads}}$ is continuously titrated under propylene epoxidation conditions, resulting in a low steady state coverage. In addition, low coverage of

adsorbed atomic O precludes the formation of oxygen induced surface reconstructions, necessary to partially lift the Ag/SO₄ reconstruction and make the active species SO_{4,ads.}[11,12]

Instrumentation

Figure 2 compares the experimentally determined photon flux of three beamlines operated by the FHI: ISISS (under operation since 2007) BEIChem beamline (under commissioning since 2018) at comparable spectral resolution under standard AP-XPS working conditions and sample position, along with CAT@EMIL. It becomes apparent that the beamline characteristics of BEIChem and ISISS nicely complement each other. The photon flux of the soft X-ray branch of EMIL (Energy Materials In-Situ Laboratory Berlin) served by the UE48 undulator at the focus position in the CAT laboratory (red line) is shown in Figure 1 as well. It is obvious that the soft EMIL beamline provides a broad photon energy range with a high photon number in the whole energy range.

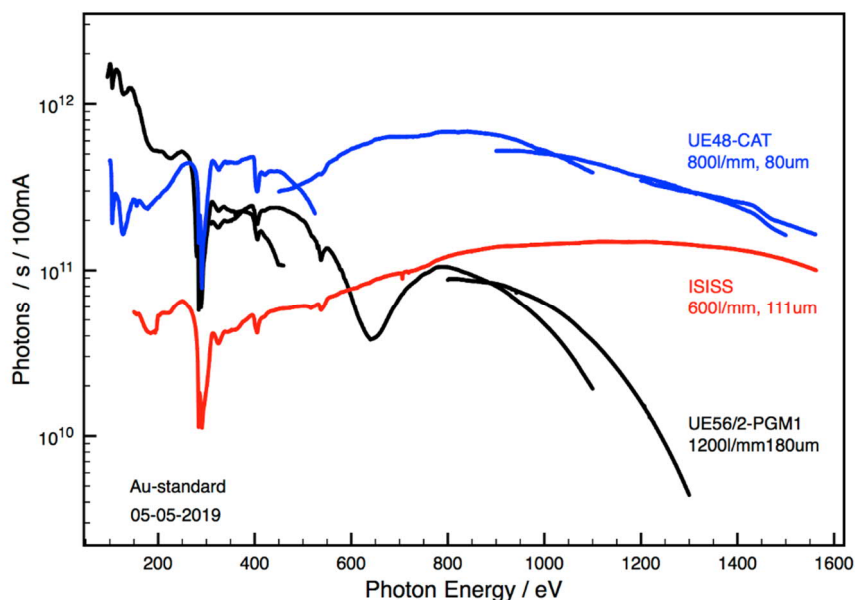


Figure 2 : Comparison of the photon flux at sample position of the soft X-ray beamlines ISISS, BEIChem (UE56/2-PGM1), and CAT@EMIL at BESSY dedicated to AP-XPS spectroscopy.

A strategy of commissioning phases combined with user experiments (e.g. within the CRC project cobalt based catalysts in isopropanol oxidation) is applied to put the CAT@EMIL facility into operation. This station combines an AP-XPS spectrometer equipped with a wide acceptance lens and high kinetic energy capabilities (up to $E_{kin}=7000\text{eV}$) with a sophisticated laboratory infrastructure optimized for in-situ XPS experiments with a chemical background. The photon

energy range will be extended to the tender X-ray regime up to 8000eV by exploiting the radiation of the cryogenic in-vacuum undulator U17 in a second installation phase of this project [13,14] in the end of 2019/beginning of 2020, hence providing a perfect match with the spectrometer specification with its broad kinetic energy range.

In summary, while the permanent user operation of the workhorse ISIS is ensured, the new AP-XPS facilities BElChem and CAT@EMIL have been put into operation step by step within the last year. All set-ups are equipped with the modular endstation/reaction cell concept developed at the FHI to optimize flexibility and possibility to adapt the instrumentation to the user needs.

References

1. Knop-Gericke, A. et al. *J. Electron Spectrosc. Relat. Phenom.* (2017), *221*, 10–17.
2. Velasco-Vélez, J. J. et al., *Surf. Sci.* (2019), *681*, 1-8.
3. Frevel, L. et al., *J. Phys. Chem. C* (2019), *123* (14), 9146–9152.
4. Mom *et al.*, *J. Am. Chem. Soc.*, (2019), *141* (16), 6537–6544.
5. Ping, Y. et al., *J. Am. Chem. Soc.* (2017), *139*, 149–155.
6. Fang *et al.*, *J. Am. Chem. Soc.*, (2010), *132*, 18214-18222.
7. Paoli *et al.*, *Chem. Sci.*, (2015), *6*, 190-196.
8. Hori, Y. et al., *Chem. Lett.* (1986), *15*(6), 897-898.
9. Kas, R., et al., *Chem. Lett.* (2014), *16*(24), 12194-12201.
10. Velasco-Velez, J. J., et al., , *ACS Sus. Chem.& Eng.* (2018) *7*(1), 1485-1492.
11. Jones, T. E., et al., *ACS Catal.* (2018), *8*(5), 3844-3852.
12. Carbonio, E. A., et al., *Chemical Science* (2018), *9*(4), 990-998.
13. Follath, R., et al., *B. J. Phys.: Conf. Series* (2013), *425*, 2120003.
14. Hendel S., et al., *AIP conference proceedings* (2016), *1741*, 030038.